

Tumbling dynamics of flexible wings

Daniel Tam* and John W.M. Bush

Department of Mathematics, Massachusetts Institute of Technology, Cambridge, MA 02139

Michael Robitaille and Arshad Kudrolli

Department of Physics, Clark University, Worcester, MA 01610

(Dated: July 14, 2009)

The influence of flexibility on the flight of autorotating winged seedpods is examined through an experimental investigation of tumbling rectangular paper strips freely falling in air. Our results suggest the existence of a critical length above which the wing bends. We develop a theoretical model that demonstrates that this buckling is prompted by inertial forces associated with the tumbling motion, and yields a buckling criterion consistent with that observed. We further develop a reduced model for the flight dynamics of flexible tumbling wings, that illustrates the effect of aeroelastic coupling on flight characteristics and explains experimentally observed variations in the wing's falling speed and range.

PACS numbers: 46.32.+x, 46.40.-f, 47.85.-g

Seed dispersal is the means by which plants expand and colonize new areas [1]. To maximize their range, some plants have developed elaborate gliding, spinning or tumbling winged seedpods, whose aerodynamics enable them to extend their flight time and range [2]. Given the absence of actuation, the efficiency of passive flight is determined by the geometry and mass distribution of the wing. It is therefore noteworthy that some gliding seedpods are thin and flexible and deform substantially during flight. We are broadly interested in elucidating the role of flexibility in passive flight. Here, we focus on the tumbling dynamics of flexible wings.

Consider a rectangular wing of uniform thickness h , width w , cross-sectional area $S = wh$, length L , density ρ_s , bending stiffness EI , falling through air of density ρ under the influence of gravity \mathbf{g} . Studies of the dynamics of freely falling rigid wings have a rich history dating back to Maxwell [3], who first gave a qualitative explanation for the observed tumbling motion of a uniformly loaded wing about its long axis. Recent work has mainly focused on the transition between the fluttering and tumbling modes, which occurs at a critical value of the parameter $I_o = \rho_s h / \rho w$ [4–7]. For small values of I_o , the wing is observed to oscillate in a side-to-side fluttering motion without net rotation. Above a critical I_o , a tumbling motion is observed, wherein the wing completes full rotations about its long axis, while drifting along an inclined trajectory (Fig. 1b). The flight properties of tumbling rigid wings have been characterized extensively through experiments [9, 10].

We consider the influence of wing flexibility on passive tumbling flight. When the wing is sufficiently long, it bends along its long axis (Fig. 1c). While previously reported [9, 10], this bending instability remains unexplained. We here demonstrate that the wing buckles under the influence of inertia, in much the same way that a beam buckles under normal compression. Buck-

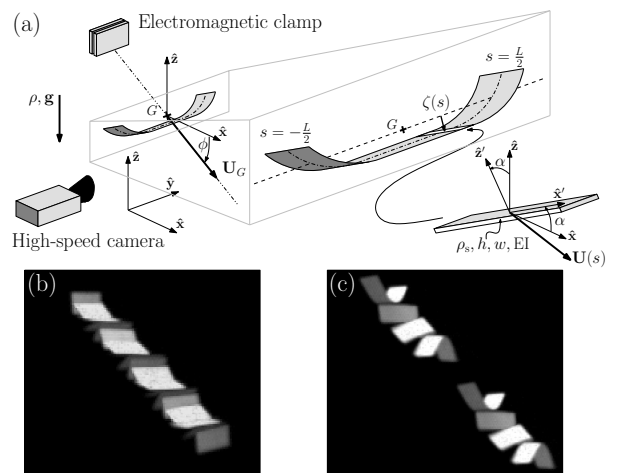


FIG. 1: (a) Schematic of the geometry of a falling, tumbling bent wing. Superimposed snapshots of a tumbling paper wing: short wings remain straight (b), while long wings bend (c). For the sake of clarity, two half cycles are shown and images are artificially spaced in (c). (See supplementary videos [8]).

ling occurs at a critical value of the transition parameter $\kappa = \sqrt[4]{\rho_s S \dot{\alpha}^2 / EI L}$, where $\dot{\alpha}$ is the rotation rate at which the wing tumbles. Note that κ prescribes the relative magnitudes of the destabilizing inertial force and the wing's resistance to bending. We proceed by elucidating the physics behind the bending of flexible tumbling wings and the manner in which elastic deformation affects the tumbling dynamics.

The bending instability of tumbling wings was investigated experimentally with rectangular paper strips of various dimensions: length L ranges between 5–28 cm, width w between 0.5–5 cm. Paper of varying surface density $\rho_s h$ were used, namely light, medium and heavy paper with $\rho_s h = 6.0, 7.5, 14 \times 10^{-2} \text{kg.m}^{-2}$ respectively. Wings are released from an electromagnetic clamp with

their leading edge parallel to the ground. We examine a parameter regime well beyond the fluttering-tumbling transition [6, 7] so that, upon release, the rectangular wings immediately start tumbling at a relatively high and constant rotation rate. Trajectories are captured by a high speed camera filming at 250 fps. Trajectories are recorded from either the front or side views and analyzed to extract the deflection amplitude Z , linear velocity U_G , rotation rate $\dot{\alpha}$ and angle of descent ϕ (Fig. 1a). Short tumbling wings remain straight (Fig. 1b), while longer ones bend symmetrically, sagging about their centerline (Fig. 1c). The transition between the two regimes appears to be sharp and depends strongly on the wing width and type of paper. Following wing bending, their shapes remain fixed and rotation rates constant to leading order. For the longest ($L > 25$ cm) and widest ($w > 3$ cm) wings, we observe both the rotation rate and the amplitude of deformation to fluctuate about their mean value by no more than 15%.

We proceed by identifying the driving force behind the bending of a tumbling wing. We assume the wing to tumble about the $\hat{\mathbf{y}}$ -axis, the trajectory to remain planar in the $(\hat{\mathbf{x}}, \hat{\mathbf{z}})$ -plane and bending to occur solely in the $(\hat{\mathbf{y}}, \hat{\mathbf{z}}')$ -plane co-rotating with the wing, in accord with experimental observations (Fig. 1). The orientation of the wing is prescribed by the pitch angle α between the horizontal $\hat{\mathbf{x}}$ and cord direction $\hat{\mathbf{x}}'$. Position along the centerline is given by the arc length s and $\zeta(s)$ denotes the deflection from the center of gravity G at a location s in the $\hat{\mathbf{z}}'$ -direction. Hence the local velocity $\mathbf{U}(s)$ can be written $\mathbf{U}(s) = \mathbf{U}_G - \dot{\alpha}\zeta(s)\hat{\mathbf{x}}'$. All equations of motion are expressed in the co-rotating reference frame $(\hat{\mathbf{x}}', \hat{\mathbf{y}}, \hat{\mathbf{z}}')$.

For small deflections, bending deformation of the free wing is governed by the linear Euler-Bernoulli equations

$$\zeta_{ssss} - \frac{\mathbf{p} \cdot \hat{\mathbf{z}}'}{EI} = 0, \quad (1)$$

with free end boundary conditions $\zeta_{ss} = 0$ and $\zeta_{sss} = 0$ at $s = \pm L/2$. \mathbf{p} is the distribution of external forces per unit length causing the wing to bend and has three components: inertial, aerodynamic and gravitational forces. It can be written $\mathbf{p}(s) = -\rho_s S \ddot{\mathbf{U}}(s) + \mathbf{L}(s) + \mathbf{D}(s) + \rho_s S \mathbf{g}$, with \mathbf{L} the local lift or aerodynamic force normal to \mathbf{U} , and \mathbf{D} the local drag or aerodynamic force antiparallel to \mathbf{U} . Because the wing is in free fall, conservation of its linear momentum requires that: $\int_{-L/2}^{L/2} \mathbf{p}(s) ds = 0$. Consequently, a simple expression for the forcing \mathbf{p} can be derived. We proceed by doing so.

Consider a wing tumbling in the straight configuration $\zeta(s) = 0$. In this case, the local velocity is constant along the wing, so inertial forces are independent of s . Furthermore, for sufficiently long wings, three-dimensional aerodynamic effects at the ends of the wing can be neglected, and the flow around the wing considered two-dimensional to leading order, which further constrains both \mathbf{L} and \mathbf{D} to be constant with respect to s . As a consequence, \mathbf{p} is

independent of s and so must indeed vanish to satisfy the conservation of linear momentum. Hence, for $\zeta(s) = 0$, the force distribution \mathbf{p} vanishes and we can deduce that the straight configuration is always a solution, albeit a potentially unstable one.

Let us now consider a bent wing, whose small deflections ζ do not vary in time, in accord with experimental observations. We seek to find the first order correction to \mathbf{p} caused by finite bending ζ . The local inertial force at arc length s now has an additional component $\rho_s S \dot{\alpha}^2 \zeta(s) \hat{\mathbf{z}}'$, and the first order correction in ζ to the aerodynamic force now scales as $\rho w \dot{\alpha} U_G \zeta(s)$, since aerodynamic pressure scales as $\rho U(s)^2$. Experimental measurements indicate that the ratio of this first order correction in inertial forces to aerodynamic forces is of order 10, which allows us to neglect the aerodynamic contribution to the correction term and consider only the inertial forces applied on the wing, hence the inertial forcing $\mathbf{p}(s) = \rho_s S \dot{\alpha}^2 \zeta(s) \hat{\mathbf{z}}'$.

The equation governing the bending dynamics (1) together with the inertial forcing forms an eigenvalue problem previously investigated in the context of fast spinning ballistic objects [11] and is similar to that arising in the Euler buckling of a beam under normal compression [12]. The general solution to the ODE (1) is a linear combination of trigonometric and hyperbolic sines and cosines. For small values of the transition parameter $\kappa = \sqrt[4]{\rho_s S \dot{\alpha}^2 / E I L}$, the trivial straight configuration, $\zeta(s) = 0$, is the only solution. However, when κ reaches a critical value, corresponding to the eigenvalue condition

$$\tan \frac{\kappa}{2} = \pm \tanh \frac{\kappa}{2} \quad (2)$$

obtained from the boundary conditions, the existence of a non-trivial solution implies that the straight configuration becomes unstable to a bent configuration through an inertial buckling transition (see detailed derivation in [8]).

The onset of instability corresponds to the smallest κ satisfying Eq. (2) $\kappa_* \approx 4.73$. κ_* characterizes either a critical buckling length for a given rotation rate, or alternatively a critical buckling rotation rate for a given length. Note that the critical rotation rate corresponds precisely to the lowest natural frequency oscillation of a free beam. The non-trivial solution to Eq. (1) at the transition is symmetrical and can be written

$$\zeta(s) = Z \frac{\cos(\frac{\kappa_*}{2}) \cosh(\frac{\kappa_*}{L} s) + \cosh(\frac{\kappa_*}{2}) \cos(\frac{\kappa_*}{L} s)}{\cos(\frac{\kappa_*}{2}) + \cosh(\frac{\kappa_*}{2}) - 2 \cos(\frac{\kappa_*}{2}) \cosh(\frac{\kappa_*}{2})}. \quad (3)$$

$Z = \zeta(0) - \zeta(L/2)$ is the total deflection of the wing and remains undetermined from the linearized equation (1). As for Euler buckling, Eq. (1) precisely predicts the transition, but leaves undetermined the details of the deflection after the transition. Nevertheless, exact shapes can be computed by solving numerically the nonlinear bending equations using the Matlab `bvp4c` routine (see detail

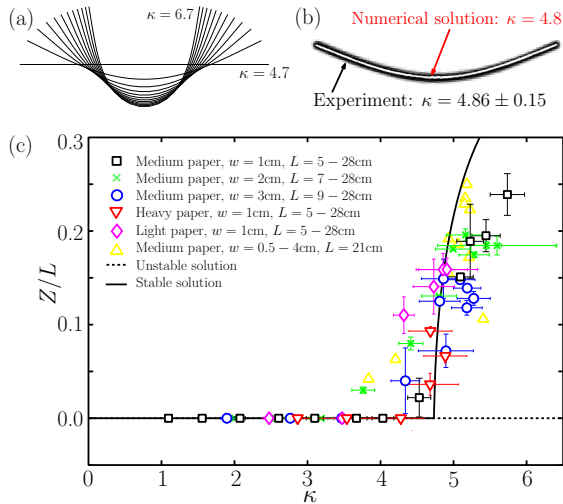


FIG. 2: (a) Computed wing shapes for $\kappa = 4.7 - 6.7$. (b) Superposition of an image of a tumbling bent wing taken from the front view and the shape computed numerically (superimposed white line). (c) Maximum wing deflection as a function of the dimensionless parameter $\kappa = \sqrt[4]{\rho_s S \dot{\alpha}^2 / EI L}$, experiments and theory (solid curve).

in [8]). Numerically computed shapes are reproduced in Fig. 2a. Note that higher order instabilities can theoretically arise for larger values of κ ; however, such high values were not achieved experimentally. For each wing, both the normalized deflection Z/L and transition parameter κ can be estimated from recordings of freely falling wings. The experimental data is reported in Fig. 2c. The maximum deflection is zero for small values of κ but increases sharply for values close to $\kappa_* \approx 4.73$, in close agreement with our numerical results (see Fig. 2c). Moreover, wing shapes observed in our experiments are compared with those computed numerically [8], and found to be in good agreement (Fig. 2b).

We now focus on flight properties of tumbling flexible wings, specifically the effect of elastic bending on the flight characteristics. A reduced model for the flight dynamics of flexible tumbling wings is developed, which consists of coupled aeroelastic equations of motion derived in nondimensional form using a characteristic length $L_{\text{ref}} = w$, mass $m_{\text{ref}} = \rho_s S L$, velocity $U_{\text{ref}} = \sqrt{\rho_s h g / \rho}$ and time $t_{\text{ref}} = L_{\text{ref}} / U_{\text{ref}}$. The scale U_{ref} is a characteristic settling speed, found by balancing gravity and aerodynamic forces. In the following, all equations are written in non-dimensional form, and we denote the non-dimensional wing length by $\Lambda = L / L_{\text{ref}}$.

We first derive a reduced equation for the bending dynamics of the wing. In non-dimensional form, Eq. (1) becomes $\ddot{\zeta} + \Omega^2 \zeta_{ssss} - \dot{\alpha}^2 \zeta = 0$, where $\Omega = \sqrt{EI / \rho_s S t_{\text{ref}} / L_{\text{ref}}^2}$ represents a non-dimensional frequency of oscillation. Substituting the solution to the linearized equations (3)

for ζ yields an equation in Z only

$$\ddot{Z} + (\omega(\Lambda)^2 - \dot{\alpha}^2) Z = 0. \quad (4)$$

This reduced equation (4) describes the dynamics of a harmonic oscillator of natural frequency $\omega(\Lambda) = \Omega \kappa_*^2 / \Lambda^2$ under inertial forcing $\dot{\alpha}^2 Z$. As expected, ω also corresponds to the lowest natural frequency for the bending oscillation of a free wing. Equation (4) captures the essential physics of the inertial buckling transition. The straight wing $Z = 0$ is always a solution, but is only stable for short wings or low rotation rates for which $\omega(\Lambda) > \dot{\alpha}$. The transition occurs for $\omega(\Lambda) = \dot{\alpha}$, which is exactly the transition criterion of Eq. (2). In this case, the total deflection need not be zero and steady solutions with finite bending are possible.

We proceed by deriving the conservation equations governing the falling motion of the wing. Similar equations have been derived for rigid wings [5–7], but these studies were aimed at characterizing the fluttering-tumbling transition, while here we only consider tumbling far from the transition and investigate the first order effect of bending. The local lift \mathbf{L} is assumed to be proportional to the circulation Γ , as predicted by quasi-steady potential flow theory, and the circulation Γ around the wing to depend only on the rotation rate $\Gamma = C_R \dot{\alpha}$, with C_R a non-dimensional parameter. The local drag \mathbf{D} is assumed quadratic in the local velocity U with constant drag coefficient C_D . Both local lift and drag depend on the local velocity and thus on the deflection ζ .

Linear momentum conservation for the entire wing is expressed in the $(\hat{\mathbf{x}}', \hat{\mathbf{z}}')$ -frame by integrating the local lift, drag and gravitational forces along the wing:

$$I_o(\dot{u} - \dot{\alpha}v) = -C_R \dot{\alpha}v - C_D U_G u - \sin \alpha, \quad (5)$$

$$I_o(\dot{v} + \dot{\alpha}u) = +C_R \dot{\alpha}u - C_D U_G v - \cos \alpha. \quad (6)$$

u and v are the components of \mathbf{U}_G in the $(\hat{\mathbf{x}}', \hat{\mathbf{z}}')$ -frame of reference and $I_o = \rho_s h / \rho w$. It bears emphasis that Eqs (5-6) are independent of the deflection ζ to first order. Since deflection is taken from the center of gravity, by definition we have $\int_{-\Lambda/2}^{\Lambda/2} \zeta(s) ds = 0$; hence, any first order correction in ζ does not contribute to a net force on the wing, as they necessarily integrate to zero.

Angular momentum conservation is expressed with respect to the center of gravity G . The only external torque acting on the wing is the aerodynamic torque, which we write as the sum of an entrainment torque that causes the wing to tumble and a dissipative torque that opposes its rotation. For a straight wing, we assume the entrainment torque to be proportional to the lift and the dissipative torque to be quadratic in $\dot{\alpha}$. For a bent wing, we also have to include the contribution from the moments of the aerodynamic forces about the center of gravity, $\int_{-\Lambda/2}^{\Lambda/2} (\dot{\zeta} \hat{\mathbf{z}}' \times (\mathbf{L} + \mathbf{D})) ds$. Now, the first order corrections in ζ to \mathbf{L} and \mathbf{D} make non-zero contributions to the

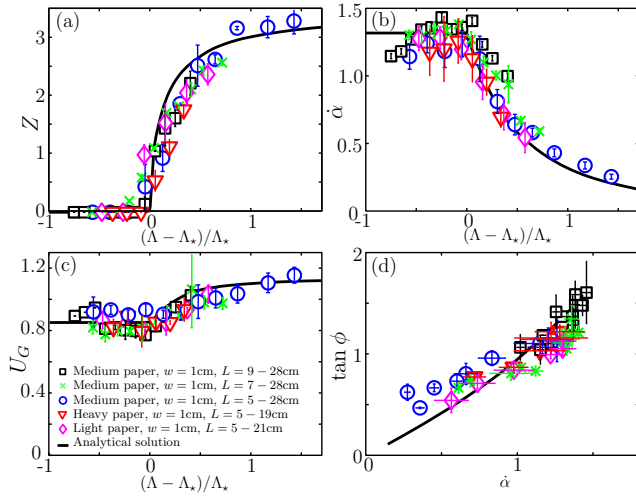


FIG. 3: Comparison between the analytical solution to our reduced model for the flight dynamics of flexible tumbling wings and experimental data of measured (a) total deflection Z , (b) linear velocity U_G and (c) rotation rate $\dot{\alpha}$ of the wing as a function of Λ/Λ_* , and (d) angle of descent $\tan \phi$ as a function of $\dot{\alpha}$.

aerodynamic torque. This contribution corresponds to an additional term in the dissipative torque proportional to $\int_{-\Lambda/2}^{\Lambda/2} \zeta(s)^2 ds$. Substituting for ζ , the solution to the linearized equations (3) yields a term that is quadratic in the total deflection Z . Hence

$$\frac{d}{dt}(J\dot{\alpha}) = \eta\dot{\alpha}U_G - \mu_1\dot{\alpha}^2 - \mu_2 Z^2 \dot{\alpha}U_G. \quad (7)$$

where J is the non-dimensional moment of inertia at G about the axis \hat{y} , and η , μ_1 , μ_2 are non-dimensional aerodynamic parameters.

The non-linear system of ODEs (4-7) is found to have a steady rotational solution for which the total deflection Z and rotation rate $\dot{\alpha}$ remain constant throughout the motion, in agreement with our experimental observations. For this solution, the ODEs (4-7) reduce to algebraic equations for Z , $\dot{\alpha}$, U_G and ϕ , that may be solved analytically. The solution depends only on one geometric parameter of the wing, its non-dimensional length Λ , and four constant aerodynamic parameters C_D , C_R , η/μ_1 , μ_2/μ_1 . Figure 3 shows the full collapse of our experimental data for the flight characteristics as functions of Λ and the good agreement with our analytical solution. Formulas for the analytic solution can be found in [8]. The aerodynamic parameters are chosen to best match the experimental data and all take reasonable values. For example, the inferred value for C_D is 0.78, lying, as expected, between the values $C_D \approx 0$ and 2 appropriate for a wing falling, respectively, parallel and perpendicular to its cord direction.

For a short wing, before the transition, no bending occurs, hence $Z = 0$ (Fig. 3a). In this regime, the analytical

solutions for $\dot{\alpha}$, U_G and ϕ of a straight wing of given cross-section correspond to constants, independent of the wing length Λ , in accord with our experimental observations and previous studies [10]. Moreover, the full collapse of the non-dimensionalized experimental data confirms that, before the transition, flight properties such as the non-dimensional rotation rate $\dot{\alpha}_*$, do not depend on the cross-sectional geometry. Therefore, the dimensional rotation rate simply scales with $1/t_{ref} \sim h^{1/2}w^{-1}$, as was first suggested in [10]. This also justifies a posteriori the scalings for the aerodynamic torques (Eq. (7)).

The transition parameter κ increases with the length Λ and the transition occurs when $\Lambda = \Lambda_* = \kappa_* \sqrt{\Omega/\dot{\alpha}_*}$. Above this critical length, Z , $\dot{\alpha}$, U_G and ϕ depend on the aerodynamic parameters and also on Λ/Λ_* . The solution can be expanded in Λ/Λ_* both around the critical point and in the limit of long wings. At the transition, the total deflection Z increases sharply as the square root of the length, but the increase is bounded and Z tends to an asymptotic value for long wings (Fig. 3a). The increased deflection causes the wing to rotate at a smaller rate, which confirms the main effect of bending on the aerodynamics, namely an increased dissipative torque that opposes rotation. The decrease in rotation rate $\dot{\alpha}$ is first linear at the transition and goes to zero asymptotically for long wings (Fig. 3b). The linear velocity on the other hand undergoes a slight increase after the transition and then reaches an asymptotic value. While moderate, the increase is confirmed by our experimental data (Fig. 3c) and implies a small increase in the descent rate. Finally, the angle of descent asymptotically decays to zero (Fig. 3d), corresponding to a decrease of range for a freely falling wing.

This study has rationalized an abrupt change in the aerodynamics of rectangular wings due to buckling, which indicates the dramatic influence of flexibility on passive flight. For tumbling wings, flexibility leads to an overall worsening of flight characteristics, with a slight increase in descent rate and decrease of range. It is thus interesting to note that tumbling seed pods of *Ailanthus Altissima* for example, do not bend as they tumble. Our study suggests a trade-off: while a lighter wing will generally have longer descent times, they may suffer a buckling instability that worsens their flight characteristics.

* Electronic address: dan_tam@math.mit.edu

- [1] R. Nathan, G. G. Katul, H. S. Horn, S. M. Thomas, R. Oren, R. Avissar, S. W. Pacala, and S. A. Levin, *Nature* **418**, 409 (2002).
- [2] S. Minamia and A. Azuma, *J. Theor. Biol.* **225**(1), 1 (2003).
- [3] J. Maxwell, *Cambridge and Dublin mathematical journal* **9**, 145 (1854).
- [4] Y. Tanabe and K. Kaneko, *Phys. Rev. Lett.* **73**, 1372

- (1994).
- [5] L. Mahadevan, C. R. Acad. Sci. Ser. IIb **323**, 729 (1996).
- [6] A. Belmonte, H. Eisenberg, and E. Moses, Phys. Rev. Lett. **81**, 345 (1998).
- [7] U. Pesavento and Z. Wang, Phys. Rev. Lett. **93**, 144501 (2004).
- [8] *Supplementary material and videos*.
- [9] P. Dupleich, NACA Technical Memorandum **1201** (1941).
- [10] L. Mahadevan, W. Ryu, and A. Samuel, Phys. Fluids **11**, 1 (1998).
- [11] T. M. Atanackovic, *Stability theory of elastic rods* (World Scientific, Singapore, River Edge, NJ, 1997).
- [12] S. Timoshenko and J. Gere, *Theory of elastic stability* (McGraw-Hill, New-York, 1961).